Continuous Precipitation Polymerization of Vinylidene Fluoride in Supercritical Carbon Dioxide: Modeling the Rate of Polymerization

Paul A. Charpentier,[†] Joseph M. DeSimone,[*,†,‡,§] and George W. Roberts[*,†,||]

Department of Chemical Engineering, North Carolina State University, Box #7095, Raleigh, North Carolina 27695-7905, and Venable and Kenan Laboratories, Department of Chemistry, University of North Carolina—Chapel Hill, CB #3290, Chapel Hill, North Carolina 27599

The kinetics of the surfactant-free precipitation polymerization of vinylidene fluoride (VF2) in supercritical carbon dioxide have been studied in a continuous stirred autoclave. Diethyl peroxydicarbonate was used as the free-radical initiator. The stirring rate and agitator design had no effect on the rate of polymerization (R_p) or on the weight-average molecular weight (M_w) of the formed poly(vinylidene fluoride) (PVDF). The fractional conversion of VF2 ranged from 7 to 26%, and R_p was as high as 27×10^{-5} mol/L·s at 75 °C and at a VF2 feed concentration of 2.5 mol/L. The PVDF polymer was collected as a dry, "free-flowing" powder and had M_w's up to 150 kg/mol and melt flow indices as low as 3.0 at 230 °C. Homogeneous, free-radical kinetics provided a reasonable basis for describing the rate of polymerization, despite the heterogeneous nature of the system. The order of the reaction with respect to the monomer was found to be 1.0, and the order with respect to the initiator was 0.5. The experimental data suggest that an inhibitor is present in the monomer or that the monomer itself acts as an inhibitor.

Introduction

Volatile organic compounds (VOCs) have been the focus of increased environmental concern and regulation since the late 1980s (e.g., the Montreal Protocol in 1987 and the Clean Air Act Amendments of 1990). Consequently, considerable effort has been devoted to finding environmentally benign solvents and processes for industrial implementation.[1] DeSimone and co-workers have shown that supercritical carbon dioxide ($scCO_2$) is a viable and promising alternative medium for free-radical, cationic, and step-growth polymerizations.[2] This work has been summarized in several recent reviews.[3−5] Indeed, DuPont intends to manufacture Teflon commercially in CO_2 by 2006.[6] There are several reasons for the intense interest in CO_2 as a polymerization medium, including the facts that CO_2 is (1) inert to highly electrophilic radicals (i.e., there is no chain transfer to solvent), (2) inexpensive ($100−200/ton), (3) of low toxicity, (4) nonflammable, and (5) environmentally and chemically benign. CO_2-based polymerization processes can lead to the elimination of (a) expensive polymer drying steps, (b) toxic and hazardous organic solvents, and (c) expensive wastewater treatment and disposal steps for removing monomers, surfactants, and emulsifiers.[7]

As industrial interest in using $scCO_2$ as a polymerization medium has grown, the need for continuous processes to harness the advantages of this medium is being recognized. A continuous system requires smaller and hence cheaper equipment for large-volume polymers. Moreover, recycling of unreacted monomer and supercritical fluid should be facilitated in a continuous system. A continuous system also can include in situ steps to purify the resultant polymer by supercritical fluid extraction[1] and to melt process the polymer in CO_2, which lowers the melt viscosity significantly.[8]

Most organic monomers and initiators are soluble in liquid and $scCO_2$,[9−11] whereas most polymers are insoluble in CO_2.[12] This behavior defines a precipitation polymerization. Continuous precipitation polymerization in $scCO_2$ should be applicable to a wide variety of industrially important monomers. We reported previously on a continuous process for the precipitation polymerization of various monomers, including acrylic acid, in $scCO_2$.[13]

Poly(vinylidene fluoride) (PVDF) is a semicrystalline, thermoplastic polymer widely used for fabricating pipe, tubing in plastic heat exchangers, column packing, valves, and pumps.[14] This polymer is produced commercially in batch reactors by either emulsion or suspension techniques, at monomer pressures of between 10 and 200 bar and temperatures from 10 to 130 °C.[15,16] In the emulsion process, the latex is coagulated, thoroughly washed, and then spray-dried to form a free-flowing powder. The suspension technique requires separation of the polymer from the water phase, thorough washing, and then drying. In both processes, large quantities of wastewater are generated and large quantities of energy are required to dry the polymer. A continuous, environmentally friendly process for PVDF manufacture would be attractive if it could eliminate the generation of waste streams and minimize the need for polymer drying. Moreover, such a process might lead to higher polymer purity by eliminating the need for additives to stabilize emulsion and suspension polymerizations.

This paper describes an effort to understand the kinetics of vinylidene fluoride (VF2) polymerization in $scCO_2$, initiated by the organic peroxide diethyl peroxydicarbonate (DEPDC). A continuous stirred autoclave reactor, which behaved as an ideal continuous stirred tank reactor (CSTR), was used. Until now, there has

* To whom correspondence should be addressed.
[†] North Carolina State University.
[‡] E-mail: desimone@unc.edu. Phone: (919) 962-2166. Fax: (919) 962-5467.
[§] University of North Carolina—Chapel Hill.
[||] E-mail: groberts@eos.ncsu.edu. Phone: (919) 515-7328. Fax: (919) 515-3465.

10.1021/ie000354z CCC: $19.00
Published on Web 10/21/2000

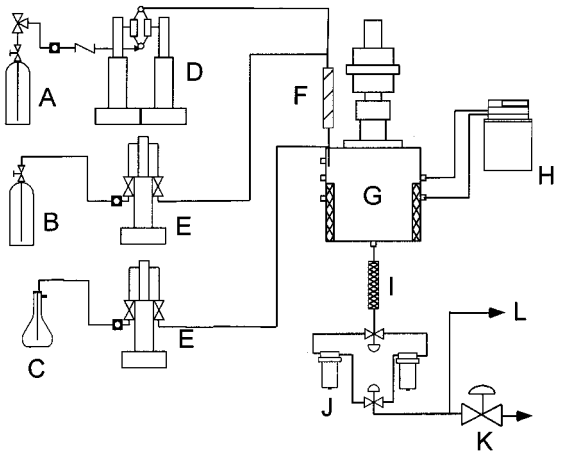

Continuous Polymerization Apparatus
A- CO2 cylinder; **B**- Monomer; **C**- Initiator Solution; **D**- CO_2 Continuous Pump; **E**- Syringe Pumps; **F**- Static Mixer; **G**- thermostated Autoclave; **H**- Chiller/Heater Unit; **I**- Heat Exchanger; **J**- Steady-State and Non-Steady-State Filters; **K**-Heated Control Valve; **L**-GC Analysis

Figure 1. Schematic of the continuous polymerization apparatus.

been very little investigation of the kinetics of free-radical polymerizations in $scCO_2$, and none of the previous studies have involved continuous operation. Moreover, very little information is available on VF2 polymerization kinetics, or on the polymerization kinetics of fluorinated monomers in general, in any medium.

We have carried out experiments in $scCO_2$ at monomer inlet concentrations ranging from 0.4 to 2.8 M, initiator inlet concentrations ranging from (8 to 50) $\times$ 10^{-4} M, temperatures ranging from 65 to 85 °C (at a constant CO_2 density of 0.74 g/mL), and mean residence times ranging from 10 to 50 min. A model for the rate of polymerization (R_p) has been developed from the experimental data.

Experimental Section

Materials. Vinylidene fluoride monomer (HFC-1132a) was generously donated by Solvay Research (Brussels, Belgium) and used without further purification. Carbon dioxide (SFE/SFC grade) was generously donated by Air Products & Chemicals, Inc. (Allentown, PA), and further purified by passage through columns containing 5A molecular sieves (Aldrich, Milwaukee, WI) and copper oxide (Aldrich) to remove excess water and oxygen, respectively. All other chemicals were obtained from Aldrich.

Initiator Synthesis. The DEPDC initiator was synthesized as previously reported, using water as the reaction medium and extracting the initiator into Freon 113 (HPLC grade).[17,18] All manipulations of the initiator were performed in an ice bath, and the final product was stored in a cold chest at −20 °C. The iodine titration technique, ASTM method E 298-91, was utilized to determine the concentration of active peroxide in the solution.

Polymerization Apparatus. Figure 1 provides a schematic of the experimental continuous polymerization apparatus. The equipment and the polymerization procedure have been described in detail elsewhere.[13] Recent modifications to the system included (a) replacing the reactor furnace with a temperature jacket (Autoclave Engineers) through which a heating/cooling fluid was circulated to provide improved temperature control, (b) addition of a countercurrent heat exchanger on the effluent line of the CSTR for cooling the exiting polymer stream to ambient temperature, and (c) addition of a gas chromatograph (GC; SRI 8610C), which sampled the exit stream (after filtration) directly through a high-performance liquid chromatograph (HPLC) valve (Valco). The GC contained a 3 ft $\times$ $^1/_8$ in. packed silica gel column, while the oven temperature was isothermal at 55 °C. Calibration of the GC was performed using CO_2 and VF2 flow rates determined by syringe pumps. Densities of VF2 and CO_2 in the cooled syringe pumps and heated reactor were determined from data provided by Solvay (VF2) and by NIST[19] (CO_2).

Polymerization Control. Polymerization took place continuously in the highly agitated 800 mL CSTR. Three streams, CO_2, VF2, and DEPDC, were fed continuously to the reactor with individual syringe pumps, while the produced polymer, as well as CO_2 and unreacted VF2 and DEPDC, left the reactor continuously. Control of the reactor temperature (T) and pressure (P) was excellent during a polymerization ($T = \pm 0.3$ °C and $P = \pm 1$ bar). Feed rates of the initiator and monomer from the syringe pumps were ±0.1%.

Polymer Collection. Collection of "steady-state" polymer normally was started after the reactor had been operating for five mean residence times by switching from one of the parallel collectors (filters), shown in Figure 1, to the other. As reported previously,[13] essentially all of the formed polymer was collected by the 1 μm filters. After each reaction, the inside of the reactor normally was coated very lightly with powder. This powder always was dry, not tacky, and could easily be wiped off the reactor walls. No sticky film formation was observed, and the wall temperature of the reactor never exceeded the melting point of the polymer.

Gel Permeation Chromatograph (GPC). All GPC measurements on the polymer samples were performed by Solvay Research (Belgium) at 40 °C on a Waters-Alliance HPLC system with 2 $\times$ HR5E and 1 $\times$ HR2E columns, using *N*,*N*-dimethylformamide (DMF) modified with 0.1 M LiBr. The GPC was calibrated at 40 °C using narrow molecular weight distribution standards of poly(methyl methacrylate) (PMMA) purchased from Polymer Laboratories Ltd.

Melt Flow Index (MFI). MFIs were determined with a Kayeness melt flow indexer at 230 °C according to the method of ASTM D-1238.

Results

Attainment of Steady State. Figure 2 shows the results obtained from GC analyses of the reactor outlet stream during a typical polymerization run. The effluent VF2 concentration was measured as a function of time onstream, expressed as a multiple of the reactor mean residence time. The mean residence time, τ, is defined as the reactor volume, V, divided by the volumetric flow rate, ν. The fractional conversions of VF2 (monomer conversions) in Figure 2 were calculated from the GC analyses. For a typical polymerization run, steady state was attained after about 5τ. Furthermore, if the reactor had been onstream for at least 5τ, the weight of the polymer collected per unit time was constant, independent of time onstream, confirming the results obtained by GC analysis.

Experimental Phase Behavior. Under the experimental conditions studied, VF2 and DEPDC were found to be miscible with CO_2, while the formed polymer powder, PVDF, was imiscible in CO_2. These studies

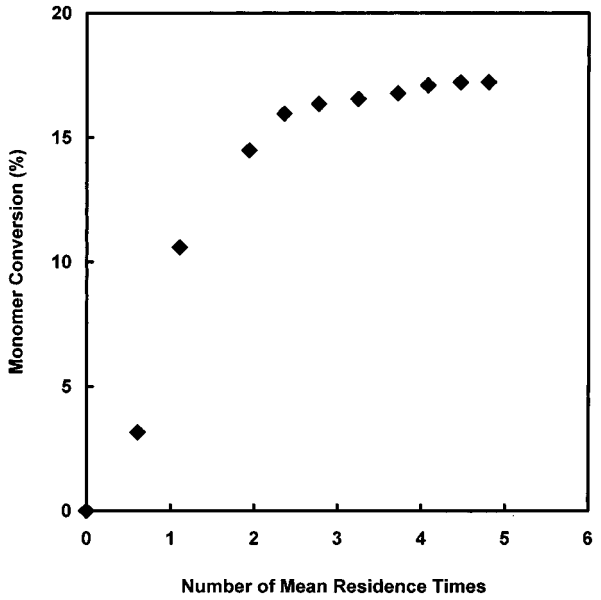

Figure 2. Approach to steady state for polymerization of VF2. Fractional conversion of VF2 versus time onstream, expressed as the number of mean residence times. The points are experimental data calculated from VF2 analyses obtained by gas chromatography. The polymerization conditions were $P = 276$ bar, $T = 75$ °C, ν_{CO_2} (volumetric flow rate of CO_2) = 26 g/min, $[VF2]_{INLET} = 0.77$ M, $[DEPDC]_{INLET} = 3$ mM, and $\tau = 21$ min.

Table 1. Parameters Characterizing the Decomposition Kinetics of Diethyl Peroxydicarbonate in Supercritical Carbon Dioxide[22]

temp, °C	k_D, $\times 10^4$ s^{-1} [a]	f [b]
65	2.4	0.61
70	4.3	0.69
75	10.3	0.59
85	35.1	0.63

[a] k_D is the first-order rate constant for the initiator decomposition. [b] The initiator efficiency, f, is the fraction of the free radicals produced by the initiator decomposition that are effective in starting polymer chains.

were performed in a variable-volume view cell, similar in design to that reported elsewhere.[1] Our observations on the solubility of PVDF in CO_2 agree with recently reported data on PVDF/CO_2 and PVDF/CH_2F_2.[20] This heterogeneous phase behavior indicates a precipitation polymerization.[21]

Residence Time Distribution (RTD) and Initiator Decomposition Studies. The RTD of the experimental reactor and the decomposition kinetics of DEPDC were determined in independent experiments, as reported elsewhere.[22] For all conditions studied, the RTD of the reactor agreed closely with that of an ideal CSTR. These experiments were performed in pure CO_2, in the absence of polymer powder.

The decomposition of DEPDC in scCO_2 obeyed a first-order rate law. Table 1 shows the initiator decomposition rate constants and the initiator efficiency.[22] No significant solvent or pressure dependence was observed for decomposition of DEPDC in scCO_2, compared to literature values using organic solvents at ambient pressures.[23] The initiator efficiency found, $f \cong 0.6$, is typical for an organic peroxide.[21] For the kinetic analysis of PVDF polymerization presented in this paper, the k_D's from Table 1 were used. A value of $f = 0.6$ was used for all temperatures studied.

Effect of Agitation on VF2 Polymerization. The first polymerization experiments dealt with the effect of agitation. Table 2 provides the effect of the stirring rate and agitator type on monomer conversion (X) and on the weight-average molecular weights (M_w). The 1.25 in. diameter Dispersimax agitator, a six-bladed Rushton-type turbine ($d/D = 0.42$), was studied from 1300 to 2700 rpm. This type of agitator provides mainly radial flow.[24] High agitation rates were studied to minimize the formation of deposits, to promote good heat transfer,[25] and to help suspend the precipitated particles. It is clear from Table 2 that the monomer conversion and M_w were not affected by the stirring rate, for the range investigated.

Table 2. Effect of Agitation on Conversion and Molecular Weight

agitation rate, rpm	agitator type[a]	monomer conv, %	$M_w \times 10^3$
1300	D	17.0	24.2
1300	U	17.3	20.3
1800	D	18.0	20.4
2300	D	17.5	
2700	D	17.7	21.2

[a] D = Dispersimax impeller. U = upward-pumping impeller.

For the lowest stirring rate, 1300 rpm, a different turbine agitator also was studied. This was a four-bladed, 45° pitch, upward-pumping agitator designed to provide a combination of axial and radial flow to help suspend the precipitated polymer particles. The conversion and M_w obtained with this agitator were the same as those with the Dispersimax impeller, indicating no effect of the agitator geometry on the polymerization, for the conditions studied. For all subsequent experiments, the Dispersimax impeller was used at a stirring rate of 1800 rpm.

The results in Table 2 indicate that the polymerization kinetics were not affected by mixing in this study. Taken in conjunction with the RTD studies that were done with pure CO_2,[22] these results support the assumption that the reactor behaved as an ideal CSTR.

Modeling the Rate of Polymerization. (i) Determination of the Monomer Order. If the inlet and outlet volumetric flow rates are equal, the mass balance for monomer around an ideal CSTR, operating at steady state, can be written as

$$R_p = \frac{[M]_{IN} - [M]_{OUT}}{\tau} \qquad (1)$$

where R_p is the rate of polymerization per unit volume, $[M]_{IN}$ is the concentration of monomer in the inlet stream, $[M]_{OUT}$ is the concentration of monomer in the outlet stream (which is the same as the concentration of monomer in the reactor for an ideal CSTR), and τ is the mean reactor residence time. For this work, $[M]_{OUT}$ was determined gravimetrically by weighing the polymer collected at steady state and was confirmed by on-line GC analysis of VF2. This allowed the R_p to be determined experimentally, because $[M]_{IN}$ and τ were known.

In "classical" free-radical polymerization, R_p is proportional to the first power of the monomer concentration and to the square root of the initiator concentration.[21] Figure 3 provides a plot of R_p versus $[VF2]_{OUT}$ for a series of experiments at 75 °C where the monomer concentration was varied over a wide range and where the inlet and outlet concentrations of DEPDC were constant. This figure illustrates that R_p is nonlinear

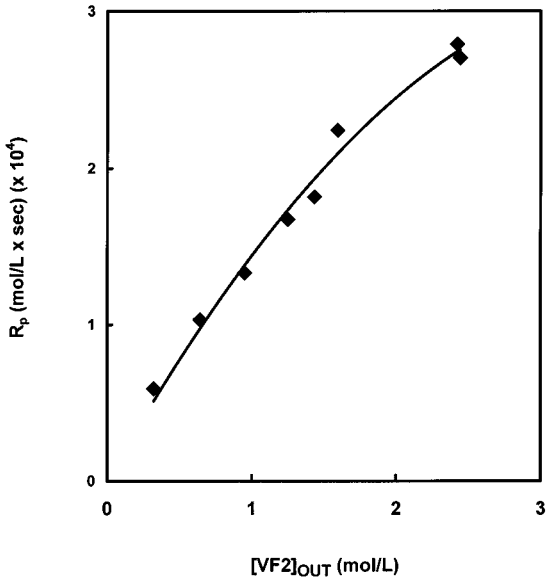

Figure 3. Rate of polymerization versus $[VF2]_{OUT}$. Test of the first-order monomer dependency. The points are experimental data fitted with a second-order polynomial. The polymerization conditions were $P = 276$ bar, $T = 75$ °C, $\nu_{CO_2} = 26$ g/min, $[DEPDC]_{OUT} = 1.3$ mM, and $\tau = 21$ min.

with the monomer concentration; the slope of the curve decreases as the monomer concentration increases.

(ii) Determination of the Initiator Order. For a CSTR at steady state, with equal inlet and outlet volumetric flow rates, the mass balance for the initiator is

$$[I]_{IN} - [I]_{OUT} - r_I\tau = 0 \qquad (2)$$

where $[I]_{IN}$ is the concentration of the initiator in the inlet stream, $[I]_{OUT}$ is the concentration of the initiator in the outlet stream, and r_I is the rate of consumption of the initiator by decomposition, per unit volume. Assuming a first-order decomposition, $r_I = k_D[I]_{OUT}$,

$$[I]_{OUT} = [I]_{IN}/(1 + k_D\tau) \qquad (3)$$

Hence, the concentration of the initiator in the reactor, $[I]_{OUT}$, can be calculated from the known inlet concentration, $[I]_{IN}$, the known mean residence time, τ, and the decomposition rate constant, k_D, as provided in Table 1.

Figure 4 is a plot of $R_p/[M]_{OUT}$ versus $[I]_{OUT}^{0.5}$, for another series of experiments where the inlet initiator concentration was varied at otherwise constant conditions. Because the initiator concentration changed, the outlet monomer concentration also varied from experiment to experiment. This plot tests both the first-order dependence on the monomer concentration and the square-root dependence on the initiator concentration. The "classical" rate model appears to apply, except for an "offset" on the x axis; i.e., the line through the data points does not go through the origin. In essence, the data suggest that a threshold initiator concentration of about 10^{-4} mol/L is required to produce a finite rate of polymerization, for the conditions shown.

Figure 4 suggests the presence of an inhibitor, and Figure 3 suggests that the inhibition effect may be associated with the monomer. The following kinetic analysis is based on the hypothesis that an inhibitor is present; this assumption will be discussed in more detail later. The model for R_p is based on the reactions shown in Scheme 1.

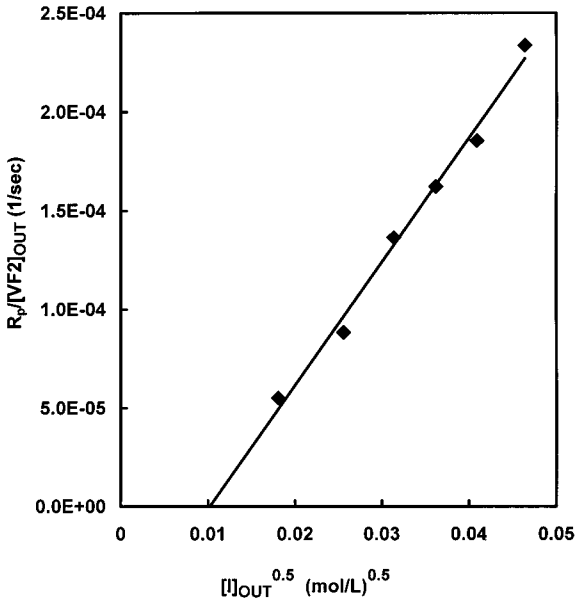

Figure 4. $R_p/[VF2]_{OUT}$ versus $[I]_{OUT}^{0.5}$. Test of the half-order initiator dependency and the first-order monomer dependency. The points are experimental data; the line is a linear least-squares fit of the points. The polymerization conditions were $P = 276$ bar, $T = 75$ °C, $\nu_{CO_2} = 26$ g/min, $[VF2]_{INLET} = 0.77$ M, and $\tau = 21$ min.

Scheme 1. Reactions for Modeling the Rate of Polymerization

(1) $I \xrightarrow{k_D} 2R^{\bullet}$ initiator decomposition

(2) $P_n^{\bullet} + M \xrightarrow{k_P} P_{n+1}^{\bullet}$ propagation

(3) $P_n^{\bullet} + P_s^{\bullet} \xrightarrow{k_T} P_{n+s}/P_n/P_s$ termination (combination and/or disproportionation)

(4) $P_n^{\bullet} + Q \xrightarrow{k_Q} P_n$ termination by inhibitor

Development of the Model Rate Equation. The rate model is based on the following assumptions: (1) the initiation, chain-growth, and termination reactions occur in the fluid phase (i.e., the rates of initiator decomposition, monomer consumption, and "dead" polymer formation in the solid polymer are negligible compared to these rates in the fluid phase), (2) the steady-state approximation (SSA) is valid, (3) rate constants are independent of the chain length, and (4) an inhibitor, Q, is present in the feed. Any free radical that might be formed in reaction 4 above is not effective in initiating new polymer chains.

The derivation of the rate model begins by applying the SSA to the total population of free radicals:

rate of initiation of chains (R_I) = rate of termination of chains (R_T)

$$2fk_D[I]_{OUT} = 2k_T[P_T^{\bullet}]^2 + k_Q[P_T^{\bullet}][Q] \qquad (4)$$

The solution to this quadratic equation is

$$[P_T^{\bullet}] = (fk_D/k_T)^{1/2}([I]_{OUT}^{1/2}\sqrt{1 + \{\beta^2/[I]_{OUT}\}} - \beta)$$

where

$$\beta = (k_Q[Q]/4k_T)/(fk_D/k_T)^{1/2} \quad (5)$$

The rate of polymerization (monomer consumption) is given by

$$R_p = k_P[M]_{OUT}[P_T^\bullet]$$

so that

$$R_p = k_P[M]_{OUT}(fk_D/k_T)^{1/2} \times ([I]_{OUT}{}^{1/2}\sqrt{1 + \{\beta^2/[I]_{OUT}\}} - \beta) \quad (6)$$

Using a series expansion for the square root term leads to

$$R_p = \alpha[M]_{OUT}\left\{[I]_{OUT}{}^{1/2}\left(1 + \frac{\beta^2}{2[I]_{OUT}} - \frac{\beta^4}{8[I]_{OUT}{}^2} + ...\right) - \beta\right\} \quad (7)$$

where

$$\alpha = k_P(fk_D/k_T)^{1/2} \quad (8)$$

If β, e.g., $k_Q[Q]$, is sufficiently small, terms that are fourth-order and higher in β can be neglected and eq 7 is approximated closely by

$$R_p/[M]_{OUT} = \alpha\{[I]_{out}{}^{1/2} - \beta + \beta^2/2[I]_{out}{}^{1/2}\} \quad (9)$$

Equation 9 is consistent with the data in Figure 4. At relatively high values of $[I]_{OUT}{}^{1/2}$, the term $\beta^2/2[I]_{OUT}{}^{1/2}$ will be small compared to β. In this region, a plot of $R_p/[M]_{OUT}$ versus $[I]_{OUT}{}^{1/2}$ will be linear, with a slope of α and an intercept of β on the x axis. This is exactly the behavior demonstrated in Figure 4. Values of α and β at 75 °C, estimated from the slope and intercept of this figure, are $\alpha = 0.0063$ L$^{0.5}$/mol$^{0.5}$•s and $\beta = 0.010$ (mol/L)$^{0.5}$. This value of β can be used to test whether the approximation involved in eq 9 is valid. For the experiments at 75 °C, the value of $[I]_{OUT}$ ranged from a low of 0.00032 mol/L to a high of 0.0022 mol/L. Thus, $\beta^2/[I]_{OUT}$ ranged from about 0.05 to 0.3, so that neglecting fourth-order and higher terms in β is reasonable.

According to eq 5, β is directly proportional to [Q], the inhibitor concentration in the CSTR. Two scenarios will be considered.

Scenario A: The inhibitor, Q, is a contaminant in the monomer feed. The word "contaminant" is used because, according to the supplier, the VF2 used in this research did not contain an inhibitor that was deliberately added to prevent reaction during shipping and storage. To simplify the following analysis, consumption of the inhibitor in the reactor is neglected, i.e., $[Q]_{OUT} = [Q]_{IN}$. This is a reasonable starting point, because the inhibitor is hypothetical at present. A more detailed analysis would require the use of a material balance on Q to relate the inlet and outlet concentrations.

Scenario B: The inhibitor is the monomer itself. This can occur, for example, if the highly electrophilic growing polymer chain, $P_n^\bullet$ in Scheme 1, abstracts a hydrogen atom from the monomer to produce a radical, $CF_2C^\bullet H$, which has a low reactivity and is inactive for practical purposes.

For scenario A, the molar ratio of Q to M in the feed is constant, so that β can be represented as

$$\beta = \gamma[M]_{IN} \quad (10)$$

where $[M]_{IN}$ is the concentration of the monomer in the feed to the reactor and γ is a proportionality constant. From eq 5,

$$\gamma = (k_Q\{[Q]/[M]_{IN}\}/4k_T)/(fk_D/k_T)^{1/2}$$

To determine whether eq 10 is obeyed, let

$$\beta' = \beta - \beta^2/2[I]_{out}{}^{1/2} \quad (11)$$

so that eq 9 becomes

$$R_p/[M]_{OUT} = \alpha([I]_{out}{}^{1/2} - \beta') \quad (12)$$

Using the estimate of α obtained from Figure 4, a value of β' was calculated for each of the experiments shown in Figure 3. To test the dependency of β on the monomer concentration postulated in eq 10, this equation can be combined with eq 11 and rearranged to yield

$$\beta'/[M]_{IN} = \gamma - (\gamma^2/2)([M]_{IN}/[I]_{OUT}{}^{1/2}) \quad (13)$$

If the model fits the experimental data, a plot of $\beta'/[M]_{IN}$ versus $[M]_{IN}/[I]_{OUT}{}^{1/2}$ will be a straight line with an intercept of γ and a slope of $\gamma^2/2$. Such a plot is provided in Figure 5A, which shows the linear dependence predicted by eq 13. A γ value of 0.016 (L/mol)$^{0.5}$ is obtained from the intercept, and a value of 0.017 (L/mol)$^{0.5}$ is obtained from the slope. The linearity of the plot, plus the excellent agreement of the values of γ calculated from the intercept and the slope, provide strong support for eq 10 and for the overall model. Data points taken with two different cylinders of monomer are shown in Figure 5A, suggesting that the concentration of the hypothetical inhibitor does not vary significantly from lot to lot.

Although Figure 5A supports the inhibitor hypothesis, the value of γ derived from this figure is based on a limited set of data. Moreover, this value will depend on the value of α that was used in the calculation of β'. In fact, the value of α used to calculate β' also was based on a limited set of data. Therefore, a more comprehensive analysis of the data was carried out. Specifically, a nonlinear regression was conducted on 17 of the 20 data points obtained at 75 °C, using eq 6 with $\beta = \gamma[M]_{IN}$. Values of α and γ that minimized the sum of the squares of the deviations between the experimental and model values of R_p were determined. These values are $\alpha = 0.0048$ L$^{0.5}$/mol$^{0.5}$•s and $\gamma = 0.0051$ (L/mol)$^{0.5}$. The value of the sum of the squares of the deviations was 1.4×10^{-9} s^{-2}.

For scenario B, the concentration of the inhibitor, Q, is equal to the concentration of VF2 in the reactor, $[M]_{OUT}$. For this case, eq 10 is replaced by

$$\beta = \delta[M]_{OUT} \quad (14)$$

where, from eq 5,

$$\delta = (k_Q/4k_T)(fk_D/k_T)^{1/2}$$

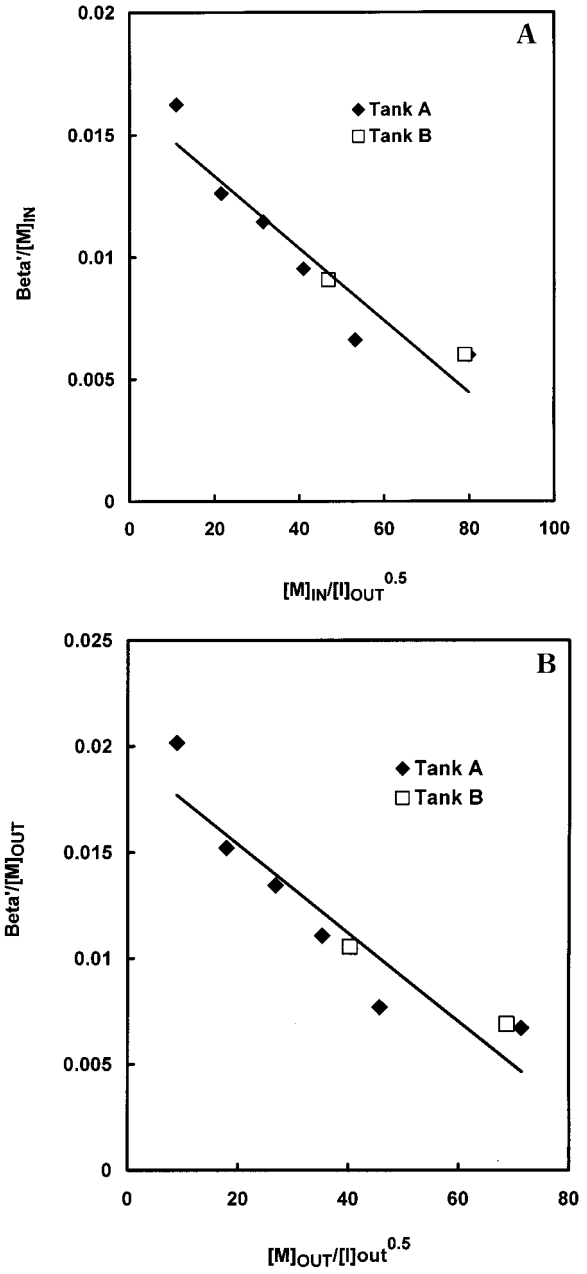

Figure 5. (A) Plot of $\beta'/[VF2]_{IN}$ versus $[VF2]_{IN}/[I]_{OUT}^{0.5}$. Test of eq 13. The points are experimental data; the line is a linear least-squares fit of the points. The polymerization conditions were the same as those shown in Figure 3. (B) Plot of $\beta'/[VF2]_{OUT}$ versus $[VF2]_{OUT}/[I]_{OUT}^{0.5}$. Test of eq 15. The points are experimental data; the line is a linear least-squares fit of the points. The polymerization conditions were the same as those shown in Figure 3.

The derivation then follows the path for scenario A, leading to

$$\beta'/[M]_{OUT} = \delta - (\delta^2/2)([M]_{OUT}/[I]_{OUT}^{1/2}) \quad (15)$$

Figure 5B is a test of eq 15. Visually, there is little difference between parts A and B of Figure 5. This is to be expected. Equation 15 is the same as eq 13, except that $[M]_{OUT}$ in eq 15 replaces $[M]_{IN}$ in eq 13. Because the fractional conversions of VF2 in these experiments were relatively low, 7−26%, the differences between $[M]_{OUT}$ and $[M]_{IN}$ were not substantial.

A nonlinear regression was carried out on the same 17 data points at 75 °C that were used in the scenario A analysis. The resulting values of α and δ were α = 0.0050 $L^{0.5}/mol^{0.5}\cdot s$ and δ = 0.0071 $(L/mol)^{0.5}$. The sum of the squares of the deviations was 1.1 × 10^{-9} s^{-2}, somewhat lower than that for scenario A. The values of α at 75 °C are essentially the same for the two scenarios.

Table 3. Values of $R_p/[M]_{OUT}$ at Different Reactor Temperatures[a]

temp, °C	$R_p/[M]_{OUT}$, ×10^4 s^{-1}	pressure, psig
65	0.58	3400
70	0.91	3700
75	1.6	4000
80	2.3	4300
85	2.5	4600

[a] Constant parameters: $[M]_{IN}$ = 0.77 M; τ = 21.2 min; $[I]_{IN}$ = 2.9 mmol/L.

Table 4. Temperature Dependence of Kinetic Parameters

Scenario A: Inhibition by Contaminant[a]

temp, °C	α, ×10^{-3} $L^{0.5}/mol^{0.5}\cdot s$	$k_p/k_T^{0.5}$, $L/mol\cdot s^{0.5}$	γ, ×10^{-3} $(L/mol)^{0.5}$
65	1.1	0.10	1.2
70	2.3	0.15	2.5
75	4.8	0.20	5.1
80	9.7	0.31	10.1
85	19.3	0.43	19.8

Scenario B: Inhibition by Monomer[b]

temp, °C	α, ×10^{-3} $L^{0.5}/mol^{0.5}\cdot s$	$k_p/k_T^{0.5}$, $L/mol\cdot s^{0.5}$	δ, ×10^{-3} $(L/mol)^{0.5}$
65	1.2	0.10	1.6
70	2.4	0.15	3.4
75	5.0	0.20	7.1
80	10.1	0.32	14.2
85	20.1	0.43	28.1

[a] E_a^α = 144 kJ/mol. E_a $(k_p/k_T^{0.5})$ = 78 kJ/mol. E_a^γ = 142 kJ/mol. [b] E_a^α = 144 kJ/mol. E_a $(k_p/k_T^{0.5})$ = 78 kJ/mol. E_a^δ = 143 kJ/mol.

Temperature Dependence. The parameters α, δ, and γ are combinations of several individual rate constants and will vary with temperature. In one series of experiments, the reactor temperature was varied from 65 to 85 °C and the reactor pressure was varied simultaneously to maintain a constant CO_2 density of 0.74 g/mL. These experiments were conducted at constant $[VF2]_{IN}$, $[IN]_{IN}$, and τ values. The resulting values of $R_p/[M]_{OUT}$ are provided in Table 3.

Nonlinear regression again was used to determine the activation energies for α and either δ or γ that minimized the sum of squares difference between the measured R_p values and those calculated from eq 6, with β given by either eq 10 or eq 14. When these calculations were carried out, α, δ, and γ at 75 °C were fixed at the previously determined values. The values of the activation energies determined by nonlinear regression are shown in Table 4, along with the value of the activation energy for $k_p/k_t^{0.5}$, which was calculated using the values of E_a^α and the activation energy for k_D, 132 kJ/mol.[22] Table 4 also contains values of α, δ, and γ at the various temperatures.

Not surprisingly, the values of E_a^γ and E_a^δ in Table 4 are very similar, about 140 kJ/mol. The values of E_a^γ are the same for scenarios A and B, i.e., 144 kJ/mol. Consequently, the activation energies for $k_p/k_t^{0.5}$ are the same for the two scenarios, 78 kJ/mol. Unfortunately, no $k_p/k_t^{0.5}$ ratios for VF2 polymerization are available in the literature against which to compare these results.

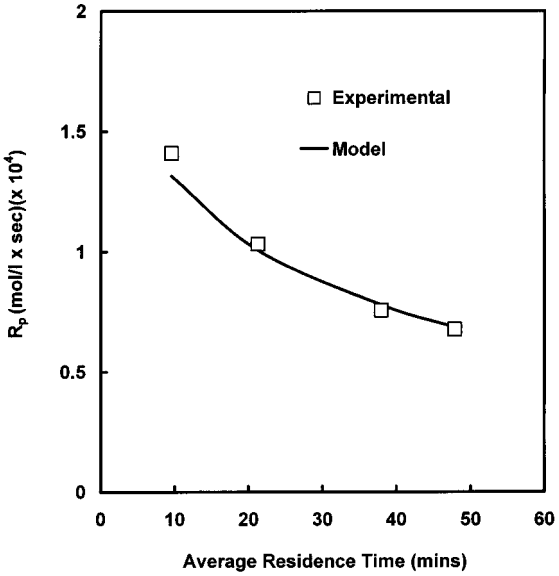

Figure 6. Effect of mean reactor residence time (τ) on the rate of polymerization (R_p). The points are experimental data. The line is eq 6 with β calculated from eq 10. The "best fit" values of α and γ at 75 °C were used in the calculations. The polymerization conditions were $P = 276$ bar, $T = 75$ °C, $\nu_{CO_2} = 26$ g/min, $[VF2]_{INLET} = 0.77$ M, and $[DEPDC]_{INLET} = 3.0$ mM.

However, the ratios in Table 4 are within the expected range of 0.01−1 for free-radical polymerizations.[26] The activation energy for $k_P/k_t^{0.5}$ obtained from these experiments is higher than the expected range of 10−40 kJ/mol.[21]

Test of the Rate Model. The effect of mean residence time, τ, was investigated over the range of 10−50 min. The flow rates of CO_2, monomer, and initiator were adjusted to give identical inlet concentrations of monomer and initiator in each experiment. Figure 6 provides the R_p values determined experimentally and compares them to those calculated from eqs 6 and 14, using the values of α and δ determined from the nonlinear regression analysis for scenario B. The data point at $\tau = 21$ min was included in the nonlinear regression; the other three data points were not included. The R_p values decrease with increasing τ, as expected, because $[VF2]_{OUT}$ and $[I]_{OUT}$ decrease with increasing τ. The experimental data follow the model equation closely, over the whole range of mean residence times investigated.

Figure 7 is a parity plot comparing the experimentally determined R_p's to those predicted from eqs 6 and 10, using the values of α and δ determined from the nonlinear regression analysis. The agreement between the experiments and the rate model is excellent.

Molecular Weight. Table 5 shows values of M_w and MFI for some of the PVDF prepared in this research and provides a comparison with commercial material prepared by suspension polymerization. The highest M_w samples prepared in this study are comparable in M_w and MFI to commercial material. Figure 8A provides a scanning electron micrograph (SEM) of the highest molecular weight PVDF powder produced during these experiments. Figure 8B shows a higher magnification of a single particle from the same sample. The SEMs of the PVDF powder suggest a relatively porous material which should offer little resistance to transport of small molecules, e.g., monomer or inhibitor, into the polymer particle.

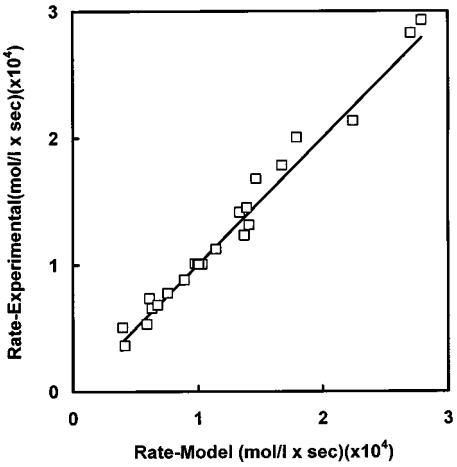

Figure 7. Parity plot showing the fit of experimental data for R_p to the rate predicted from eqs 6 and 10, with the "best fit" values of α and γ at 75 °C and the "best fit" values of E_a^α and E_a^γ.

Table 5. Melt Flow Indices (MFIs) of PVDF Samples

sample no.	M_w (GPC)	MFI temp, °C	MFI, g/10 min
several	15 000−47 000	170	400−0.5
31	150 000	230	2.6
commercial	>195 000	230	1.4

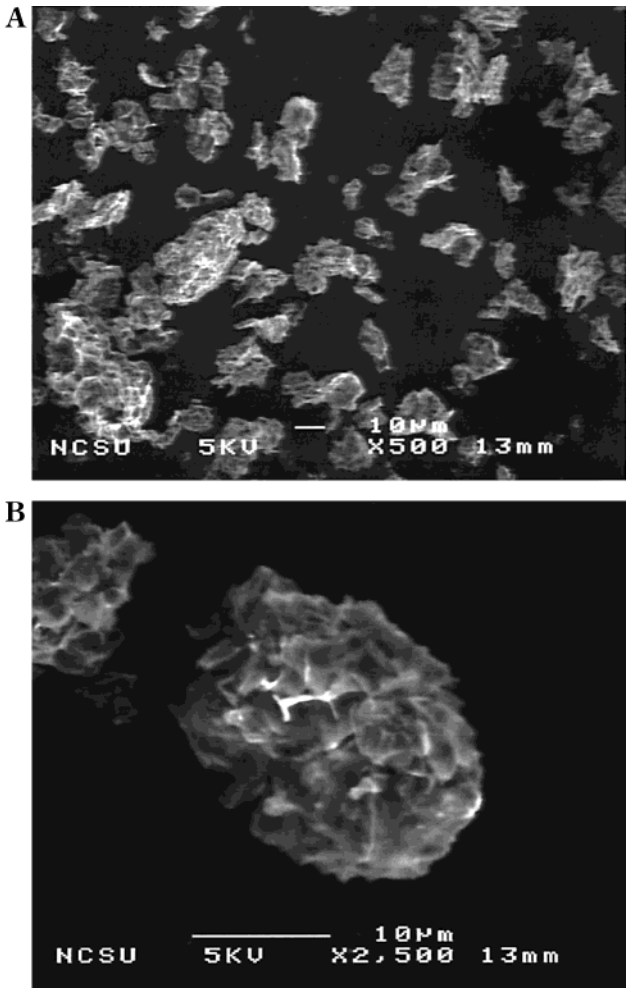

Figure 8. SEM of PVDF powder: (A) low magnification; (B) high magnification.

Discussion

The kinetic model for VF2 polymerization presented above contains two features that warrant further dis-

cussion: (a) the fact that a homogeneous (single-phase) model accurately describes the rate of polymerization and (b) the inhibition effect that appears to be associated with the monomer. Unfortunately, the literature provides very little insight into either feature.

The only reported kinetic data for VF2 polymerization were obtained in solution.[27] Acetone, ethyl acetate, and methyl acetate were used as solvents, and the initiator was bis(4-*tert*-butylcyclohexyl) peroxydicarbonate. Monomer orders were found approaching 1.8 and the initiator orders approximated the classical value of 0.5, with relatively small differences between the three solvents.

Several heterogeneous polymerizations, e.g., vinyl chloride and acrylonitrile, often show initiator orders exceeding the classical value.[28] This behavior has been attributed to polymer radicals precipitating in the nonsolvent environment to form tightly coiled chains which "trap" or "occlude" the radicals. These trapped radicals can react with monomer, but the bimolecular termination reaction is slowed considerably, leading to autoacceleration and apparent initiator orders greater than 0.5. However, radical trapping in precipitation polymerizations decreases with increasing temperature and is normally insignificant above 60 °C.[28] Relatively high temperatures were used in this study, i.e., 65−85 °C, so occlusion should be minimal. Autoacceleration was not observed in these experiments, as evidenced by the decrease in R_p with increasing τ, as shown in Figure 7.

Because PVDF essentially is insoluble in $scCO_2$, a polymer particle should precipitate after a relatively small number of monomer units have been added. However, the kinetics of precipitation are unknown. It may be that the lifetime of a single chain is short compared to the time required for that chain to precipitate. In other words, the time required for initiation, growth, and termination of a polymer molecule may be short compared to the time required for precipitation. Even if the time scales for chain growth and precipitation are comparable, the kinetics of chain growth may appear to be homogeneous if the radical end of the polymer chain protrudes into the fluid phase after precipitation.

Despite the apparent success of the present homogeneous kinetic model, the possibility of a parallel polymerization in the solid polymer particles cannot be excluded. We have reported previously that pressure has no significant effect on the decomposition of the DEPDC initiator used in this study.[22] However, pressure may have two competing effects on heterogeneous polymerization kinetics: (a) increasing pressure decreases the free volume of the polymer through a hydrostatic effect, and (b) increasing pressure increases sorption of CO_2, which increases the free volume of the polymer. Poly(vinylidene fluoride) has been found to be more influenced by the latter effect. Plasticization by the $scCO_2$ leads to increased free volume and chain mobility.[29] This argument, plus the micrographs of Figure 8, suggests that polymerization could continue inside the particles, if radicals were present and if the concentration of monomer were sufficiently high. A study to measure the partition coefficients for VF2 and DEPDC between the solid PVDF and the supercritical fluid is underway in our laboratory.[30] This study should shed additional light on the locus of polymerization and the extent to which it can be "tuned" by adjusting the pressure of $scCO_2$ and/or the concentration of monomer.

It is important to emphasize that the exact nature of the inhibition effect seen in these experiments remains undefined. The mechanism of a reaction can never be proven solely through kinetic analysis. Chromatographic analyses of the monomer and the $scCO_2$ have not provided any evidence to support the hypothesis of a "foreign" inhibitor. The fact that the strength of the inhibition effect did not change when the supply of the monomer was changed lends some support to scenario B, in which the inhibition effect is attributed to chain transfer to the monomer, with the formation of an unreactive radical. In fact, the picture of scenario B is consistent with the known chemistry of VF2 polymerization. The predominant end of the growing polymer chains is $-C^{\bullet}F_2$.[31] It is quite reasonable that this highly electrophilic radical can chain transfer to vinylidene fluoride by abstracting a hydrogen, because the more reactive the chain end, the greater the rate of chain transfer to the monomer.[21] Once formed, the $CF_2C^{\bullet}H$ radical should be essentially unreactive because it is stabilized by the electronegative CF_2 group. A study of the composition of the polymer chain ends via ^{19}F NMR, which is underway in our laboratory, may help to resolve the issue of inhibition by the monomer.

The molecular weight data for the polymers produced in these experiments will be the subject of a subsequent paper. The analysis of these data should also contribute to the understanding of the relative importance of polymerization in the fluid and polymer phases.

The conversions and molecular weights achieved in this study are lower than what might be considered reasonable for industrial practice. However, the kinetic model that has been developed provides a sound basis for adjusting reactor operation to obtain higher conversions and molecular weights, e.g., through different initiators, monomer concentrations, temperatures, and reactor residence times.

Conclusions

Polymerization of VF2 in $scCO_2$ is heterogeneous, i.e., a precipitation polymerization. Nevertheless, a model based on homogeneous chain growth provided an excellent description of the polymerization kinetics. The observed order of the reaction with respect to the initiator was 0.5, and the order with respect to the monomer was 1.0. However, an inhibition step had to be included in the reaction mechanism to account for an "offset" in the polymerization rate. The stirring rate and agitator design had no effect on the rate of polymerization. The conversion of VF2 in these polymerizations ranged from 7 to 26%, and the rate of polymerization (R_p) reached a maximum of 27×10^{-5} mol/L·s at a VF2 feed concentration of 2.5 mol/L at 75 °C. The PVDF polymer was collected as a dry, "free-flowing" powder and had M_w's of up to 150 kg/mol.

Acknowledgment

This work was supported in part by Solvay Advanced Polymers, Inc., through the Kenan Center for the Utilization of Carbon Dioxide in Manufacturing and in part by the STC Program of the National Science Foundation under Agreement No. CHE-9876674. We thank Solvay Research, Belgium, for performing GPC analyses of the PVDF samples. We extend special

thanks to Dr. Roland Martin of Solvay Research, Belgium, for many helpful suggestions and insightful criticisms.

Literature Cited

(1) McHugh, M. A.; Krukonis, V. J. *Supercritical Fluid Extraction*: *Principles and Practice*, 2nd ed.; Butterworth-Heinemann: Boston, 1994.

(2) DeSimone, J. M.; Guan, Z.; Elsbernd, C. S. Synthesis of Fluoropolymers in Supercritical Carbon Dioxide. *Science* **1992**, *257*, 945−947.

(3) Kendall, J. L.; Canelas, D. A.; Young, J. L.; DeSimone, J. M. Polymerizations in Supercritical Carbon Dioxide. *Chem. Rev.* **1999**, *99*, 543−563.

(4) Canelas, D. A.; DeSimone, J. M. Polymerizations in Liquid and Supercritical Carbon Dioxide. *Adv. Polym. Sci.* **1997**, *133*, 103−140.

(5) Shaffer, K. A.; DeSimone, J. M. Chain Polymerizations in Inert Near and Supercritical Fluids. *Trends Polym. Sci.* **1995**, *3*, 146−153.

(6) McCoy, M. DuPont, UNC R&D effort yields results. *Chem. Eng. News* **1999**, 10.

(7) Baker, R. T.; Tumas, W. Toward Greener Chemistry. *Science* **1999**, *284*, 1477−1478.

(8) Kwag, C.; Manke, C. W.; Gulari, E. Rheology of Molten Polystyrene with Dissolved Supercritical and Near-Critical Gases. *J. Polym. Sci., Part B*: *Polym. Phys.* **1999**, *37*, 2771−2781.

(9) Hyatt, J. A. Liquid and Supercritical Carbon Dioxide as Organic Solvents. *J. Org. Chem.* **1984**, *49*, 5097−5101.

(10) O'Shea, K. E.; Kirmse, K. M.; Fox, M. A.; Johnston, K. P. Polar and Hydrogen-Bonding Interactions in Supercritical fluids. Effects on the Tautomeric Equilibrium of 4-Phenylazo-1-Naphthol. *J. Phys. Chem.* **1991**, *95*, 7863.

(11) Bartle, K. D.; Clifford, A. A.; Jafar, S. A.; Shilstone, G. F. Solubilities of Solids and Liquids of Low Volatility in Supercritical Carbon Dioxide. *J. Phys. Chem. Ref. Data* **1991**, *20*, 728.

(12) McHugh, M. A.; Krukonis, V. J. In *Encyclopedia of Polymer Science and Engineering*, 2nd ed.; Mark, H. F., Bikales, N., Overberger, C. G., Menger, G., Kroschwitz, J. I., Eds.; John Wiley & Sons: New York, 1989; Vol. 16.

(13) Charpentier, P. A.; Kennedy, K.; DeSimone, J. M.; Roberts, G. W. Continuous Polymerizations in Supercritical Carbon Dioxide: Chain-Growth Precipitation Polymerizations. *Macromolecules* **1999**, *32*, 5973−5975.

(14) Dohaney, J. E. Poly(Vinyledene Fluoride). In *Kirk−Othmer Encyclopedia of Chemical Technology*, 4th ed.; Kroschwitz, J. I., Ed.; John Wiley & Sons: New York, 1994; Vol. 11, pp 694−712.

(15) Dohany, J. E.; Humphrey, J. S. In *Encyclopedia of Polymer Science and Engineering*; Mark, H. F., Bilkales, N. M., Overberger, C. G., Menges, G., Eds.; Wiley: New York, 1989; Vol. 17.

(16) Russo, S.; Pianca, M.; Moggi, G. In *Poly(vinylidene fluoride)*; Salamone, J. C., Ed.; CRC: Boca Raton, FL, 1996; Vol. 9.

(17) Mageli, O. L.; Sheppard, C. S. *Organic Peroxides*; Wiley-Interscience: New York, 1970.

(18) Hiatt, R. *Organic Peroxides*; Wiley-Interscience: New York, 1970; Vol. II.

(19) Lemmon, E. W.; McLinden, M. O.; Friend, D. G. In *NIST Chemistry WebBook, NIST Standard Reference Database Number 69*; Mallard, W. G., Linstrom, P. J., Eds.; National Institute of Standards and Technology: Gaithersburg, MD, 1998.

(20) Lora, M.; Lim, J. S.; McHugh, M. A. Comparison of the Solubility of PVF and PVDF in Supercritical CH_2F_2 and CO_2 and in CO_2 with Acetone, Dimethyl Ether, and Ethanol. *J. Phys. Chem. B* **1999**, *103*, 2818−2822.

(21) Odian, G. *Principles of Polymerization*, 3rd ed.; John Wiley & Sons: New York, 1991.

(22) Charpentier, P. A.; DeSimone, J. M.; Roberts, G. W. Decomposition of Polymerisation Initiators in Supercritical CO_2: A Novel Approach to Reaction Kinetics using a CSTR. *Chem. Eng. Sci.* Accepted for publication.

(23) Dixon, D. W. *Decomposition Rates of Organic Free Radical Initiators*. In *Polymer Handbook*; Brandrup, J., Immeregut, E. H., Grulke, E. A., Eds.; John Wiley & Sons: New York, 1999; Vol. II, pp 1−76.

(24) Geankoplis, C. J. *Transport Processes and Unit Operations*, 3rd ed.; Prentice Hall: Englewood Cliffs, NJ, 1993.

(25) Gerrens, H. How to Select Polymerization Reactors, Part II. *CHEMTECH* **1982**, July, 434−443.

(26) Kamachi, M.; Yamada, B. In *Polymer Handbook*, 4th ed.; Brandrup, J., Immergut, E. H., Grulke, E. A., Eds.; John Wiley & Sons: New York, 1999.

(27) Russo, S.; Behari, K.; Chengji, S.; Pianca, M.; Barchiesi, E.; Moggi, G. Synthesis and microstructural characterization of low-molar-mass poly(vinylidene fluoride). *Polymer* **1993**, *34*, 4777−4781.

(28) Bamford, C. H. In *Encyclopedia of Polymer Science and Engineering*; Mark, H., Ed.; John Wiley & Sons: New York, 1988; Vol. 13, pp 708−867.

(29) Briscoe, B. J.; Lorge, O.; Wajs, A.; Dang, P. Carbon Dioxide−Poly(Vinylidene Fluoride) Interactions at High Pressure. *J. Polym. Sci., Part B*: *Polym. Phys.* **1998**, *36*, 2435−2447.

(30) Kennedy, K. A.; Roberts, G. W.; DeSimone, J. M. Continuous Precipitation Polymerization of Vinylidene Fluoride: Phase Equilibrium Properties. Poster presented at the International Symposium on Supercritical Fluids, Atlanta, GA, April 8−12, 2000.

(31) Cais, R. E.; Kometani, J. M. Polymerization of vinylidene fluoride-d.2. Minimal regiosequence and branch defects and assignment of preferred chain-growth direction from the deuterium isotope effect. *Macromolecules* **1984**, *17*, 1887−1889.

Received for review March 15, 2000
Revised manuscript received June 26, 2000
Accepted June 26, 2000

IE000354Z